

Studies of solid state electrochromic devices based on PEO/siliceous hybrids doped with lithium perchlorate

P. C. Barbosa^a, M. M. Silva^{a,*}, M. J. Smith^a, A. Gonçalves^b, E. Fortunato^b

^a*Centro de Química, Universidade do Minho, Gualtar, 4710-057 Braga, Portugal*

^b*Centro de Investigação de Materiais, Universidade Nova de Lisboa, Campus da FCT 2829 - 516 Caparica, Portugal*

* E-mail address: nini@quimica.uminho.pt

Abstract

Sol-gel hybrid organic-inorganic networks, doped with a lithium salt, have been used as electrolytes in prototype smart windows. The work described in this presentation is focused on the application of these networks as dual-function electrolyte/adhesive components in solid-state electrochromic devices. The performance of multi-layer electrochromic devices was characterized as a function of the choice of precursor used to prepare the polymer electrolyte component and the guest salt concentration. The prototype devices exhibited good open-circuit memory, coloration efficiency, optical contrast and stability.

Keywords: Solid polymer electrolytes; Sol-gel; Electrochromic materials; Tungsten oxide

1. Introduction

During the last two decades a remarkable international research effort has been dedicated to the development of solvent-free solid polymer electrolytes based on poly(ethylene oxide) [1-8]. The most probable applications of these materials are in primary and secondary lithium batteries [7] or electrochromic windows [9]. Thin films of electrochromic materials deposited onto transparent conductive surfaces provide the basis of variable light transmission through controlled electrochemical oxidation or reduction.

Applications in windows with adjustable light transmission for use in automotive and aeronautic vehicles and houses have already been proposed [10, 11].

In recent years, the sol-gel method has been successfully used for the production of various novel organic-inorganic frameworks with tunable characteristics [12-15]. The intense activity in this sub-domain of solid-state research is motivated by advantages of tailoring advanced multifunctional compounds by mixing organic and inorganic components at the nano-dimension level in a single material [14-17]. The synergy of this combination and the specific role of the internal organic-inorganic interfaces enhances the range of application of nanohybrid materials in areas such as electrochemistry, biology, mechanics, ceramics, electronics and optics [14, 15]. The hybrid concept is well-adapted to the production of advanced solid-state materials presenting ion-conducting properties, with the advantage of replacing viscous liquid systems by solid or rubbery materials [16-19].

Electrochromic materials are able to change their optical properties in a reversible manner over a large number of coloration/bleaching cycles as a result of the application of a voltage pulse. These materials are of interest as components of displays, rear-view mirrors, smart windows and time-elapse labels. Many polymers are soluble in common organic solvents and can be deposited as thin films, permitting the construction of low-cost devices with large display surfaces. In this presentation the use of sol-gel techniques to prepare thin electrolyte films containing LiClO_4 dissolved in diureasil matrices is described.

2. Experimental details

2.1. Sample preparation

Host networks of organically modified silicates (ormosils), prepared from oxyethylene chains of controlled lengths grafted onto siloxane groups through urea bridges (di-ureasils), have been designated as d-U(2000) and d-U(900). In agreement with traditional terminology [20,

21], electrolytes were identified using the $d\text{-U}(2000)_n\text{LiClO}_4$ notation. In this system $d\text{-U}(2000)$ indicates the average molecular weight of the host framework and n expresses the salt content as the number of ether oxygen atoms per Li^+ cation. Known amounts of lithium perchlorate were incorporated into host matrices, forming di-ureasils with compositions of $200 \geq n \geq 0.5$.

Lithium perchlorate (LiClO_4 , Aldrich, 99.99%), α,β -diamine poly(oxyethylene-co-oxypropylene) (Jeffamine ED-2001®, Fluka, average molecular weight 2001 gmol^{-1}) and O,O' -bis(2-aminopropyl) polyethylene glycol (Jeffamine ED-900®, Fluka, average molecular weight 900 gmol^{-1}) were dried under vacuum at 25°C for several days. The bridging agent, 3-isocyanatepropyltriethoxysilane (ICPTES, Aldrich 95 %), was used as received. Ethanol ($\text{CH}_3\text{CH}_2\text{OH}$, Merck, 99.8%) and tetrahydrofuran (THF, Merck, 99.9%) were dried over molecular sieves prior to use. High purity distilled water was used in all experiments.

Transparent conductive oxide: gallium doped zinc oxide films (ZnO:Ga) were deposited on glass substrates by r.f. (13.56 MHz) magnetron sputtering using a ceramic oxide target ($\text{ZnO:Ga}_2\text{O}_3$ (95:5 wt%)), SCM, Suffern, NY, USA). Sputtering was carried out at room temperature, with an argon flow of 20 sccm and a deposition pressure of 0.11 Pa. The substrate/target separation was 10 cm and the rf power was held constant at 175 W [22]. Electrochromic films of tungsten oxide (WO_3) were prepared by thermal evaporation using WO_3 pellets (SCM, 99.99% purity) at 1.2×10^{-3} Pa and at a rate of 1.03 nm/seg.

The synthesis of LiClO_4 -doped di-ureasils has been described in detail elsewhere [20, 21]. The procedure used for $d\text{-U}(900)_n\text{LiClO}_4$ involved grafting a diamine containing approximately 15.5 oxyethylene repeat units onto the ICPTES precursor, to yield the di-urea cross-linked hybrid precursor. This material was subsequently hydrolyzed and condensed in the sol-gel stage of synthesis to induce the growth of the siloxane framework. Xerogels with n greater than 5 were obtained as flexible transparent, monolithic films with a yellowish hue, whereas compounds with $n = 1$ and 0.5 were rather brittle, powdery agglomerates.

2.2. Sample characterization

2.2.1. Impedance spectroscopy

Total ionic conductivities of ormolytes were determined by impedance measurements carried out at frequencies between 96kHz and 500mHz with a Solartron 1250 FRA and 1286 ECI. Electrolyte samples were located between two 10 mm diameter ion-blocking gold electrodes (Goodfellow, > 99.95%) to form a symmetrical cell which was secured in a constant-volume support [23] installed in a Buchi TO51 tube oven. Measurements of conductivity were effected during heating cycles between 20 and 90°C. A calibrated type K thermocouple was used to measure the sample temperature with a precision of about $\pm 0.2^\circ\text{C}$. Repeated conductivity measurements confirmed that reproducibility was better than 5%. A typical impedance spectra is illustrated in Figure 1.

2.2.2. Thermal analysis

Samples cut from dry films were transferred to 40 μL aluminium cans within a dry argon-filled glovebox. Analysis was carried out under flowing argon with a Mettler DSC 821e, using a heating rate of $5^\circ\text{C}\cdot\text{min}^{-1}$ between 25 and 300°C. Thermogravimetric studies were effected using a Rheometric Scientific TG1000 thermobalance operating under a flowing argon atmosphere. A heating rate of $10^\circ\text{C}\cdot\text{min}^{-1}$ was used with all samples.

2.2.3. Electrochemical stability

Electrochemical stability of electrolytes was evaluated within a dry argon-filled glovebox using a two-electrode cell configuration. Surface polishing of a 25 μm diameter gold microelectrode was completed outside the dry-box and the electrode was washed and dried before transfer into the dry-box. Cell assembly was initiated by locating a clean lithium disk counter electrode (Aldrich, 99.9%, 10mm diameter, 1mm thick) on a stainless steel current

collector. A sample of electrolyte was centered on the counter electrode and cell assembly was completed by supporting the microelectrode in the centre of the electrolyte disk. An Autolab PGSTAT-12 (Eco Chemie) was used to record voltammograms at a scan rate of 100mVs^{-1} . Measurements were conducted at room temperature within a Faraday cage located inside a glovebox.

2.2.4. Device assembly and characterization

Device assembly was carried out by spreading a small sample of electrolyte on the surface of a ZnO:Ga/WO₃ coated glass substrate using a spinner rotating at 2000 rpm for 40 s. Typical coating thicknesses were 200 nm (ZnO:Ga) and 300 nm (WO₃). A second ZnO:Ga coated plate was placed on top of the electrolyte layer. Optical transmission measurements were obtained using a Shimadzu-3100 UV–Vis–NIR double beam spectrophotometer in the wavelength range from 300 to 900 nm [22]. The choice of coloring and bleaching voltages applied to the assembled devices was based on a series of exploratory experiments. In these experiments the device response was observed as the voltage limits were progressively increased. The objective was to determine the conditions under which a rapid device response was obtained while preserving an acceptable cycle life. The maximum range of potential limits applied was from -4.0 to 4.0 V.

3. Results and Discussion

3.1. Conductivity

The ionic conductivity of the electrolytes was measured as a function of salt composition and temperature. The objective of this characterization was to identify the electrolyte with the most favorable behaviour for use as a component of the electrochromic display. In general, salts with a polarizing cation and a large anion with a well-delocalized charge, and therefore also with a low lattice energy, are the most suitable for use in polymer

electrolytes [7]. In spite of the dangers associated with the anion, LiClO_4 is a salt that satisfies the conditions mentioned above and provides good electrolyte behaviour, relative to the d-U(900) di-ureasils doped with lithium triflate, LiCF_3SO_3 [24]. Figure 2 illustrates the variation of total ionic conductivity of the d-U(900)_n LiClO_4 electrolyte as a function of temperature. This data also demonstrates the non-linear variation of conductivity with temperature in the range between 25 and 100 °C. The inset graph reveals the conductivity maximum at $15 \geq n \geq 8$ and at temperatures above 30°C. For compositions with high salt content ($n < 8$) the total ionic conductivity decreases, particularly at lower temperatures.

Figure 3 is included to demonstrate the effect of the choice of ureasil networks on the ionic conductivity. The Arrhenius plots show the variation of ionic conductivity with temperature of selected compositions of the U(2000), U(900) and U(600) di-ureasils [25]. As expected, U(600)-based ormolytes are less conducting than the other di-ureasils, because the oxyethylene segments of U(600) are very short, restricting the chain mobility necessary to transport the guest ions. The higher molecular weight chains of the doped U(900) and U(2000) di-ureasils were found to support higher conductivity [26, 27].

3.2. Thermal analysis

From the DSC analysis of the d-U(900)_n LiClO_4 di-ureasils it was possible to conclude that these materials are completely amorphous over the range of temperatures studied. The onset of thermal decomposition was estimated from thermogravimetric analysis. The upper limit of the application of di-ureasils incorporating LiClO_4 is effectively determined by the guest salt concentration. The results presented in Figure 4 show a decrease in thermal stability with increasing salt concentration, confirming that the salt has a destabilizing influence on the hybrid matrix host. The highest decomposition temperature of 283°C was registered for the $n = 200$ composition, a value similar to that observed for the d-U(2000)_n LiClO_4 di-ureasil [25]. The difference in behaviour of di-ureasils U(2000) and U(900) doped with LiClO_4 is also

clear in Figure 4, where for $n < 25$ compositions, the $d\text{-U}(900)_n\text{LiClO}_4$ di-ureasils show a much lower thermal stability (209°C) than the corresponding $d\text{-U}(2000)_n\text{LiClO}_4$ electrolytes [25]. Differences between $\text{U}(2000)$ and $\text{U}(900)$ networks may arise, for example, as a consequence of the presence of catalyst or stabilizer residues in the manufacturer's formulation. In spite of their moderate thermal stability, these materials are appropriate for use in a variety of technological applications at ambient or close-to-ambient temperatures.

The ionic mobility of charged species in a polymer electrolyte is to a large extent determined by the mobility of the polymer host segments [7]. As expected from previous studies of similar oxyethylene/siloxane electrolytes [25, 28], an increase in salt concentration causes a corresponding increase in T_g of the $d\text{-U}(900)_n\text{LiClO}_4$ di-ureasils (Figure 5). The poor mechanical properties of the compositions with the highest salt content ($n = 0.5$ and $n = 1$) limit the practical usefulness of the electrolyte in the sense that the electrolyte performs inadequately as a device component. It is interesting to observe that the T_g of electrolytes based on the di-ureasil matrix is almost constant (-50°C) in samples with $n \geq 40$. This observation suggests that the oxyethylene chains of the $d\text{-U}(900)_n\text{LiClO}_4$ are not involved in the coordination of the lithium ions in this range of composition. Figure 5 also shows that for compositions with $n \leq 40$ the presence of guest ionic species does not affect the $d\text{-U}(2000)$ matrix host so significantly as in the case of the $d\text{-U}(900)_n\text{LiClO}_4$ compositions.

3.3. Electrochemical stability

The electrochemical stability range of the lithium-doped di-ureasils was determined by microelectrode cyclic voltammetry over the potential range between -1.25V and 5.5V . The potential limit for the electrolyte system corresponds to the value at which a rapid rise in current was observed and where the current continued to increase as the potential was swept in the same direction. The overall stability of electrolytes was excellent, with no electrochemical oxidation occurring at anodic potentials less than about 4.5V versus Li/Li^+ .

Figure 6 shows a typical voltammogram of an electrolyte samples of d-U(900)₈LiClO₄ composition.

3.4. Electrochromic device operation

The scheme in Figure 7 shows the structure of the prototype electrochemical device characterized in the preliminary experiments reported herein. The optical behaviour of the display was reproducible and superior to that observed with comparable devices employing conventional liquid electrolytes, particularly with respect to the stability of the electrochromic material. We observed that the initial value of the luminous transmittance in devices with polymer electrolytes was also slightly higher than that of comparable devices with liquid electrolytes. This may be due to the significant reduction of the electrolyte layer thickness made possible through the use of the polymeric component. Leakage performance, memory effect and humidity deterioration were also notably improved. The results presented in Figure 8 report the optical transmittance in the wavelength range 300-900 nm for the devices based on d-U(2000)_nLiClO₄ and d-U(900)_nLiClO₄ di-ureasils. It is clear that the best results are obtained for compositions with high ionic conductivity. In the case of the d-U(2000)_nLiClO₄ and d-U(900)_nLiClO₄ di-ureasils the electrolyte compositions are $20 < n < 40$ and $8 < n < 15$, respectively. While these exploratory results are encouraging it is obviously necessary to optimize device assembly procedures and further improve mechanical and conductivity performance of the electrolyte layer to demonstrate the full potential of sol-gel derived solid polymer electrolytes as multifunctional components.

Table 1 summarizes the average transmittance and optical density exhibited by devices. The average transmittance in the visible region of the spectrum was above of 68% for all the samples analyzed. After coloration the devices assembled with d-U(2000)₂₀LiClO₄ and d-U(900)₈LiClO₄ di-ureasils present an average transmittance of 44% and an optical density

of 0.30. All the devices under analysis presented good stability and may be of interest for application in smart windows (Figure 9).

4. Conclusion

In this work novel di-ureasil d-U(900) and d-U(2000) composites incorporating LiClO_4 guest salt were investigated and used as dual-function components in prototype devices. These electrolytes were obtained as amorphous films, with excellent mechanical adaptation and adhesion to the electrode surface and good electrochemical and thermal stability. These materials provide significant advantages in optical performance, cycle lifetime and durability of the electrochromic device relative to conventional liquid electrolytes. In general, the use of solid polymer electrolytes may be expected to improve leakage performance, memory effect and humidity resistance. In addition, the sol-gel processing strategy provides ready access to materials with a greater precision of structural control than that of traditional methods of polymer synthesis. Appropriate alterations in the sol-gel procedure may permit progressive improvements in the mechanical and conductivity behaviour of the electrolyte component. The encouraging initial results obtained with electrochromic smart windows based on di-ureasil matrices doped with LiClO_4 , provide motivation for future optimization studies.

Acknowledgments

The authors are pleased to acknowledge the support provided by University of Minho and the *Fundação para a Ciência e Tecnologia* (contracts POCI/QUI/59856/2004, POCTI/CTM/48853/2002, POCTI/3/686, SFRH/BD/22707/2005) for laboratory facilities. M. M. Silva gratefully acknowledges the *Fundação Oriente* for travel funds.

References

- [1] B.E. Fenton, J.M. Parker, P.V. Wright, *Polym.* 14 (1973) 589.
- [2] P.V. Wright, *Br. Polym. J.* 7 (1975) 319.
- [3] M.B. Armand, J.M. Chabagno, M.J. Duclot, in: *Proceedings of the 2nd International Meeting on Solid Electrolytes*, St. Andrews, 1978 (Extended abstract 6.5.1).
- [4] C.A. Vincent, *Prog. Solid. St. Chem.* 17 (1987) 145.
- [5] M. Armand, *Faraday Discuss. Chem. Soc.* 88 (1989) 65.
- [6] B. Scrosati, *Proceedings of the 2nd International Symposium on Polymer Electrolytes*, Elsevier Applied Science, Amsterdam, 1990.
- [7] a) F.M. Gray, *Solid Polymer Electrolytes: Fundamentals and Technological Applications*, VCH Publishers, Inc, New York, 1991; b) F.M. Gray, *Polymer Electrolytes*, RSC Materials Monographs, Royal Society of Chemistry, London, 1997; c) M.B. Armand, in: J.R. MacCallum and C.A. Vincent (Eds.), *Polymer Electrolyte Reviews*, Vol 1, Elsevier, London 1987.
- [8] *Proc. 6th International Symposium on Polymer Electrolytes*, Kanagawa, Japan, 1-6 Nov., 1998; *Electrochim. Acta* 45 (2000).
- [9] B. Scrosati, *Applications of Electroactive Polymers*, Chapman and Hall, London, 1994.
- [10] T. Kase, M. Kawai, M. Ura, *SAE Technical Paper Series*, 861362 (1986).
- [11] C.M. Lampert, *Materials Today* 7 (2004) 28.
- [12] C.J. Brinker, G.W. Scherer, *Sol-Gel Science: The Physics and Chemistry of Sol-Gel Processing*, Academic Press, London, 1990.
- [13] P. Gomez-Romero, C. Sanchez, *Functional Hybrid Materials*, Wiley Interscience, New York, 2003.
- [14] P. Judeinstein, C. Sanchez, *J. Mater. Chem.* 6 (1996) 511.
- [15] C. Sanchez, F. Ribot, B. Lebeau, *J. Mater. Chem.* 9 (1999) 35.

- [16] V. de Zea Bermudez, C. Poinssignon, M. Armand, *J. Mater. Chem.* 7 (1997) 1677.
- [17] P. Judeinstein, J. Livage, A. Zarudiansky, R. Rose, *Solid State Ionics* 28 (1988) 1722.
- [18] M. Armand, *Adv. Mater.* 2 (1990) 278.
- [19] B. Orel, U.O. Krasovec, U.L. Stangar, *J. Sol-Gel Sci. Technol.* 11 (1998) 87.
- [20] L.D. Carlos, V. de Zea Bermudez, M.C. Duarte, M.M. Silva, C.J. Silva, M.J. Smith, M. Assunção, L. Alcácer, in: C. Ronda, T. Welker (Eds.), *Physics and Chemistry of Luminescent Materials VI*, Vol. 97-29, Electrochemical Soc. Proc., San Francisco, 1998, p. 352.
- [21] V. de Zea Bermudez, L.D. Carlos, M.C. Duarte, M.M. Silva, C.J. Silva, M.J. Smith, M. Assunção, L. Alcácer, *J. Alloys and Compounds* 21 (1998) 275.
- [22] V. Assunção, E. Fortunato, A. Marques, A. Gonçalves, I. Ferreira, H. Águas, R. Martins, *Thin Solid Films* 442 (2003) 102.
- [23] C.J.R. Silva, M. J. Smith, *Electrochim. Acta* 40 (1995) 2389.
- [24] M.M. Silva, V. de Zea Bermudez, L.D. Carlos, M.J. Smith, *Electrochim. Acta* 45 (2000) 1467.
- [25] M.M. Silva, S.C. Nunes, P.C. Barbosa, A. Evans, V. de Zea Bermudez, M.J. Smith, D. Ostrovskii, *Electrochimica Acta*, in press.
- [26] C. Berthier, W. Gorecki, M. Minier, M.B. Armand, J.M. Chabagno, P. Rigaud, *Solid State Ionics* 11 (1983) 91.
- [27] S.M. Gomes Correia, V. de Zea Bermudez, M.M. Silva, S. Barros, R.A. Sá Ferreira, L.D. Carlos, A.P. Passos de Almeida, M.J. Smith, *Electrochimica Acta* 47 (2002) 2421.
- [28] S.C. Nunes, V. de Zea Bermudez, M.M. Silva, S. Barros, M.J. Smith, E. Morales, L.D. Carlos, J. Rocha, *Solid State Ionics* 176 (2005) 1591.

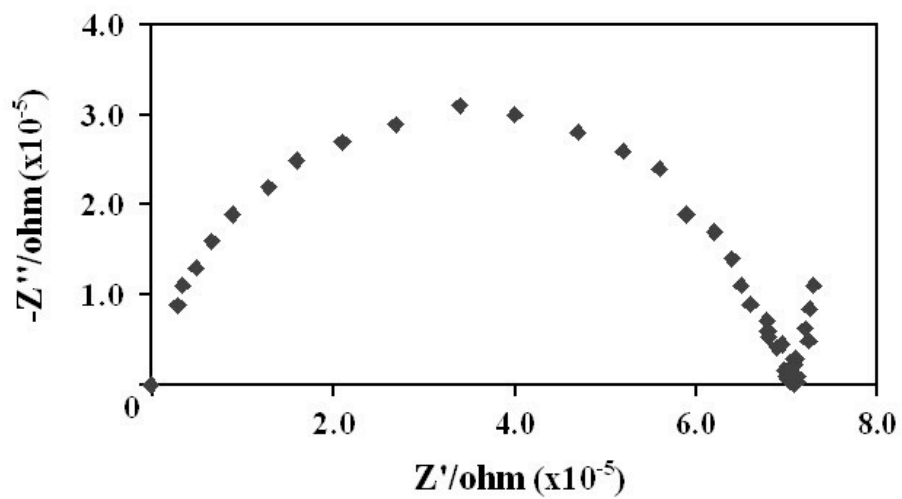


Fig.1. AC impedance spectra of a d-U(900)₈LiClO₄ electrolyte sample at 41.7°C

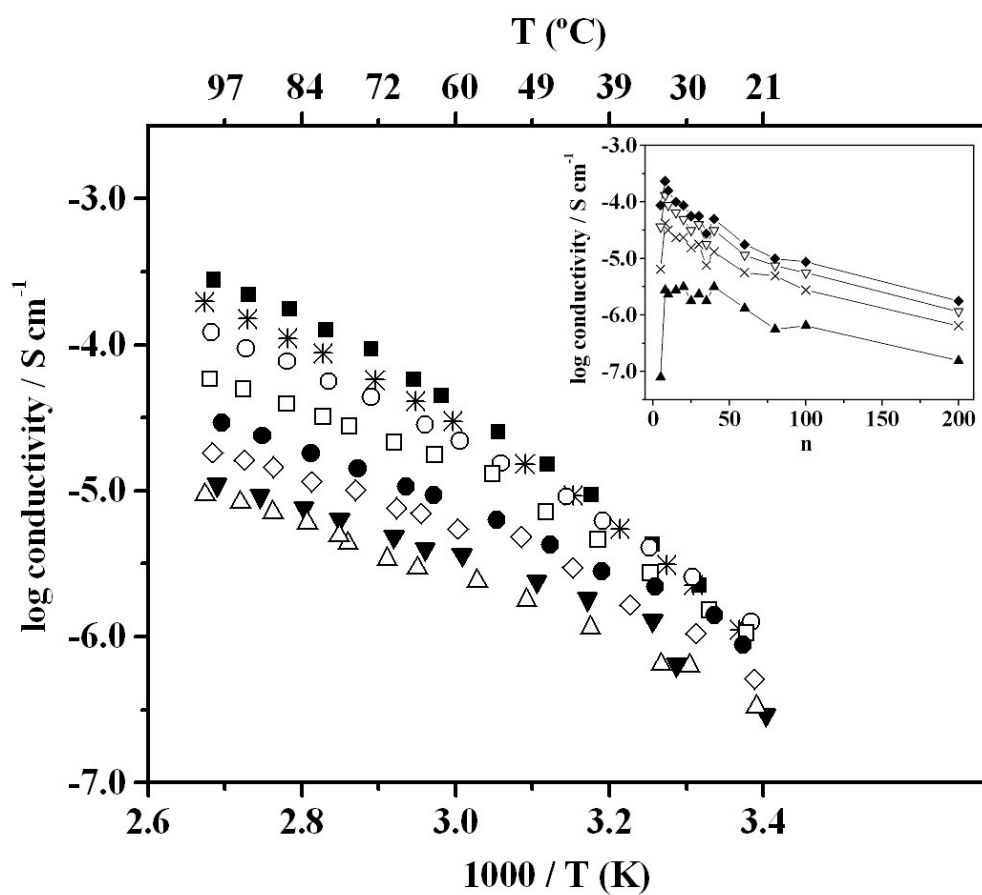


Fig. 2. Variation of conductivity of selected d-U(900)_nLiClO₄ di-ureasils with temperature ($n = 8$ ■, 10 *, 15 ○, 25 □, 35 ●, 60 ◇, 80 ▼ and 100 △). Inset shows conductivity isotherms (30°C ▲, 60°C ×, 80°C ▽ and 95°C ◆).

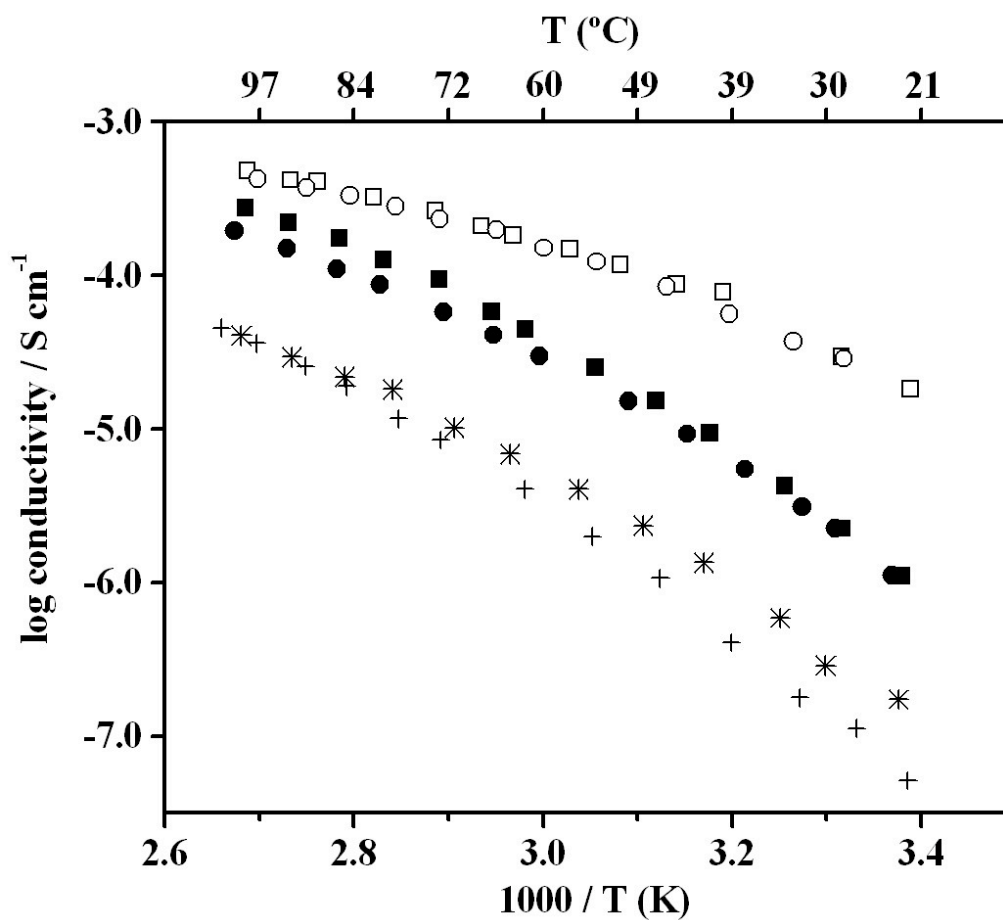


Fig. 3. Comparison of ionic conductivity between d-U(2000)_nLiClO₄, d-U(900)_nLiClO₄ and d-U(600)_nLiClO₄ di-ureasils (U(2000)₂₀LiClO₄ □, U(2000)₃₀LiClO₄ ○, U(900)₈LiClO₄ ■, U(900)₁₀LiClO₄ ●, U(600)₁₀LiClO₄ *, U(600)₅LiClO₄ +).

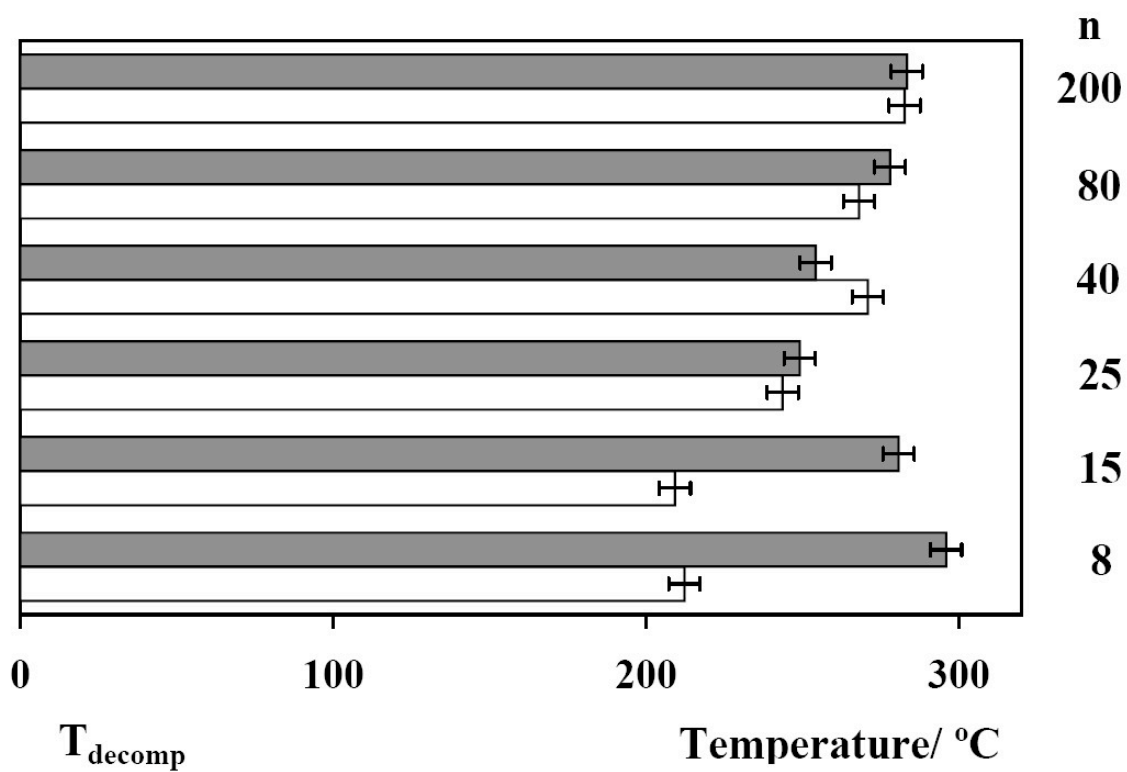


Fig. 4. Extrapolated onset of degradation temperatures from TGA results: white rods – $d\text{-U}(900)_n\text{LiClO}_4$, grey rods – $d\text{-U}(2000)_n\text{LiClO}_4$. The error bars indicate a precision of about $\pm 4^\circ\text{C}$ on all measurements.

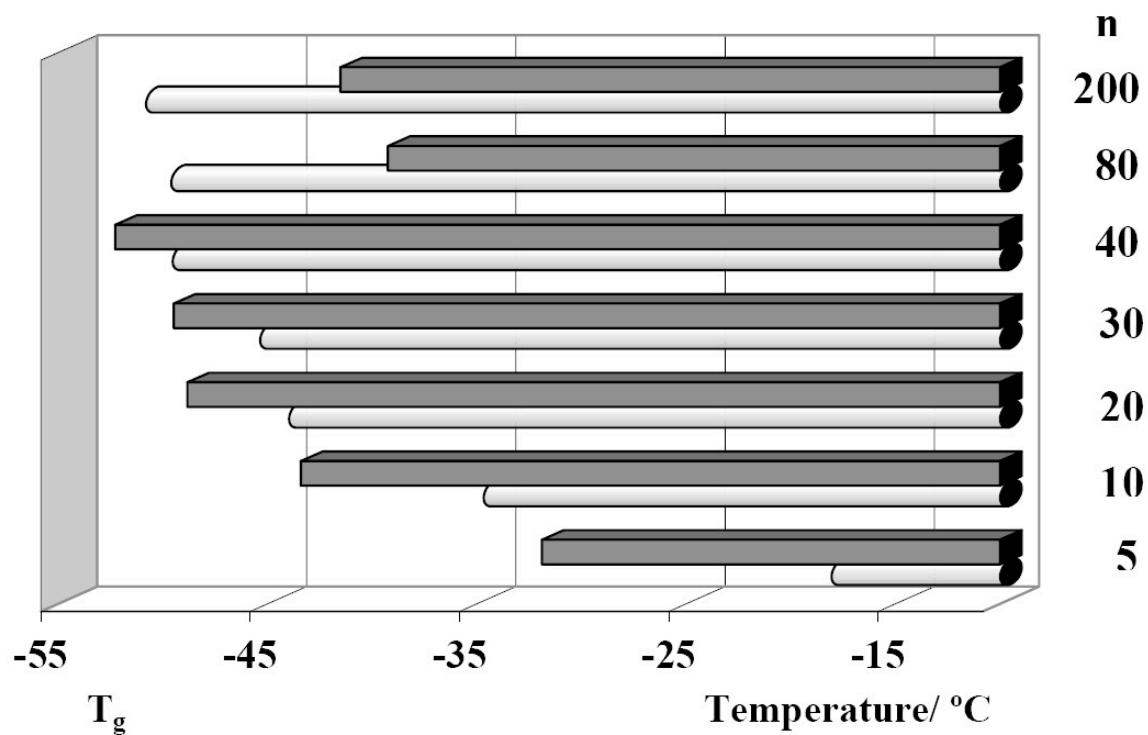


Fig. 5. Extrapolated onset of glass transition temperatures of di-ureasils: oval rods – $d-U(900)_nLiClO_4$, rectangular rods – $d-U(2000)_nLiClO_4$. The precision of these values is estimated at $\pm 0.5^\circ C$.

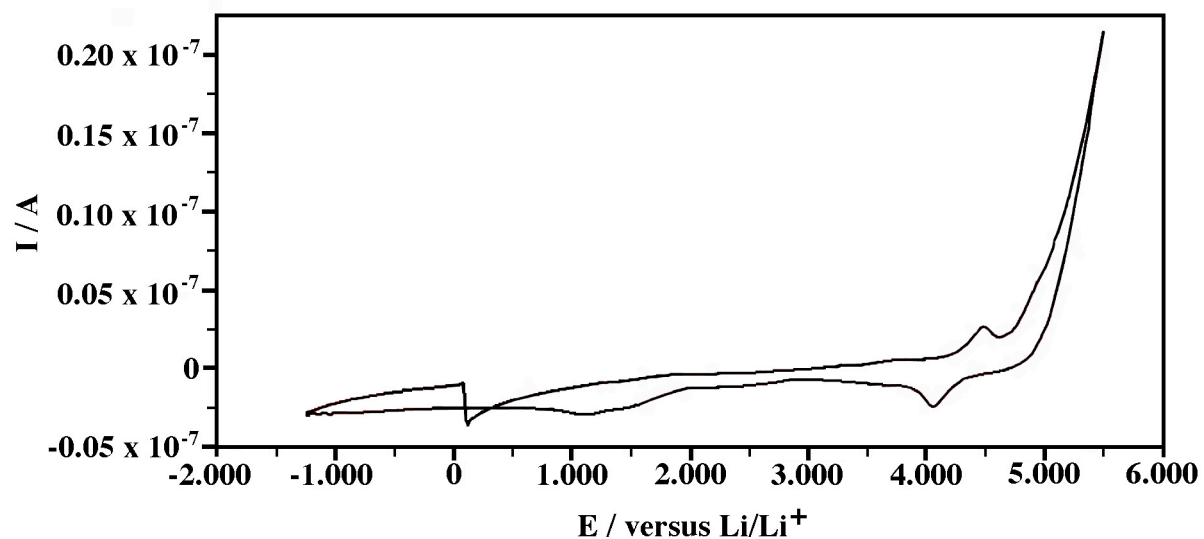


Fig. 6. Voltammogram of d-U(900)₈LiClO₄ electrolyte at a 25 μm diameter gold microelectrode vs Li/Li⁺. Initial sweep direction is anodic and sweep rate is 100 mVs⁻¹.

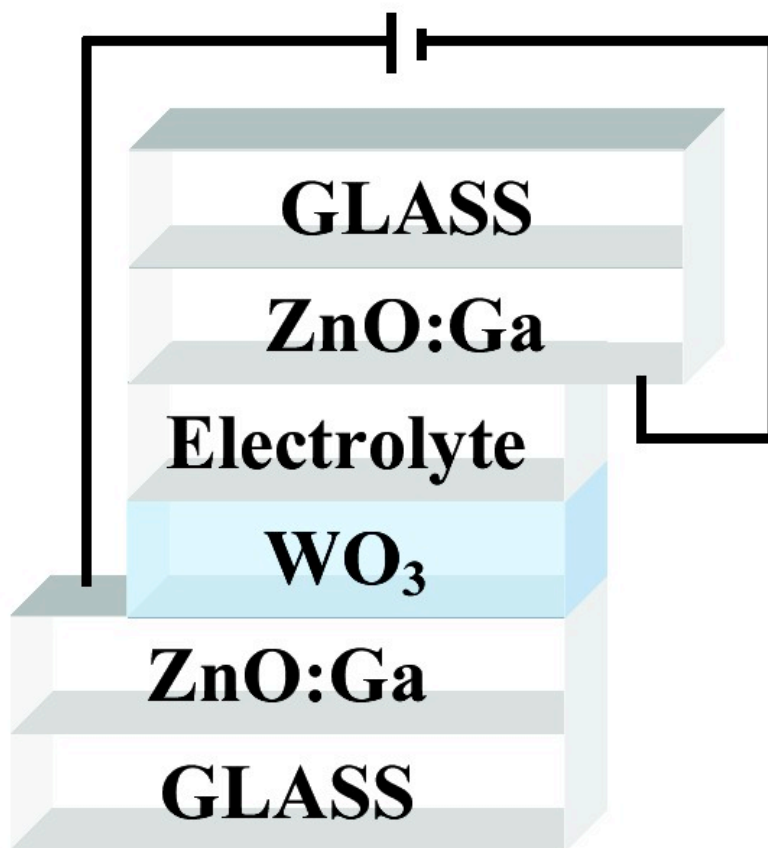


Fig. 7. Schematic illustration of the prototype electrochromic device structure.

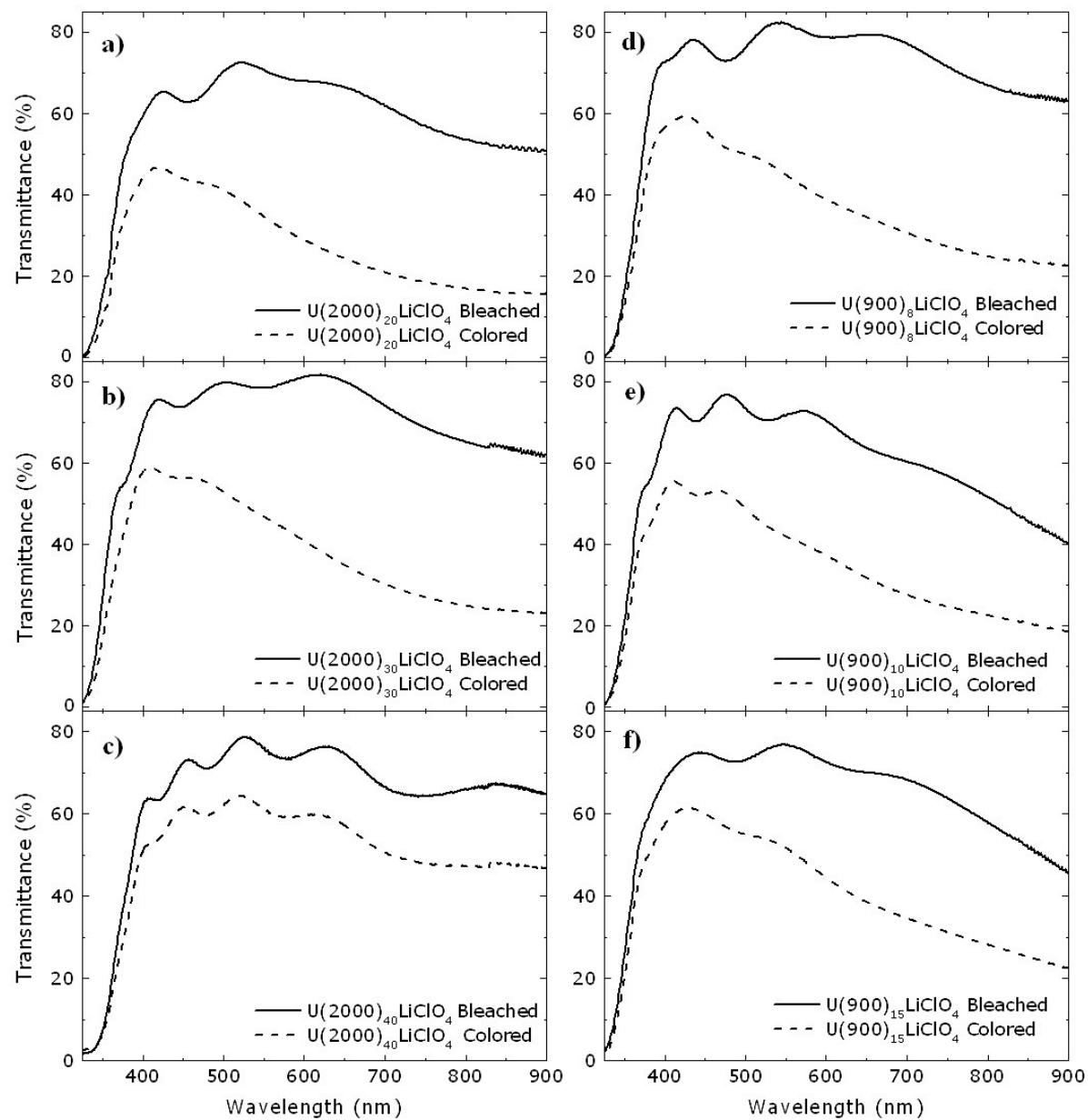


Fig. 8. Optical transmittance as a function of wavelength for the electrochromic device in bleached and colored state using (a) d- $U(2000)_{20}LiClO_4$; (b) d- $U(2000)_{30}LiClO_4$; (c) d- $U(2000)_{40}LiClO_4$; (d) d- $U(900)_8LiClO_4$; (e) d- $U(900)_{10}LiClO_4$; (f) d- $U(900)_{15}LiClO_4$.

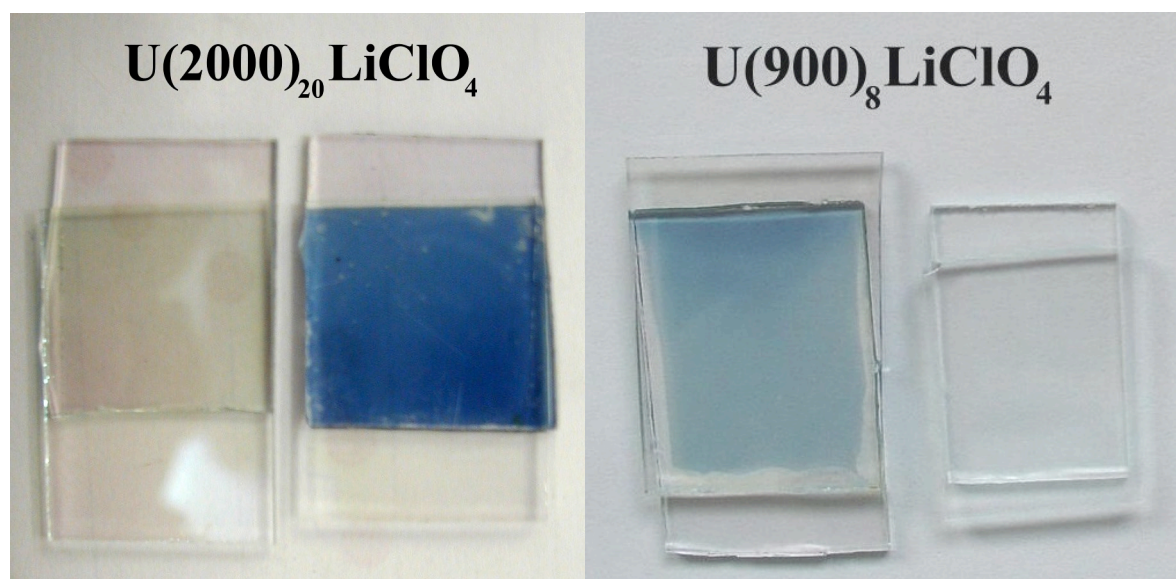


Fig. 9. Electrochromic device in bleached and colored states for compositions with highest ionic conductivity.

Table 1

Average transmittance and optical density exhibited by electrochromic devices.

Sample	Transmittance in bleached state (%)	Transmittance in colored state (%)	Optical density
U(2000) ₂₀ LiClO ₄	68.84	44.50	0.30
U(2000) ₃₀ LiClO ₄	78.90	57.23	0.23
U(2000) ₄₀ LiClO ₄	75.80	61.84	0.09
U(900) ₈ LiClO ₄	68.40	44.45	0.30
U(900) ₁₀ LiClO ₄	74.40	54.40	0.24
U(900) ₁₅ LiClO ₄	75.90	58.05	0.17